THERMAL DESTRUCTION OF A GLASS/PHENOLIC COMPOSITE

Michael L. Hobbs, James T. Nakos, and Patrick D. Brady
Sandia National Laboratories, Engineering Sciences Center, Albuquerque, NM 87185 USA

Introduction

Predicting the response of phenolic materials to fire is important for safety analysis. This paper summarizes a thermal decomposition model developed for MXB-71, a phenolic material made using a nylon resin with chopped half-by-half inch glass fabric [1,2]. The thermal response of MXB-71 was measured using thermogravimetric analysis (TGA), differential scanning calorimetry (DSC), and laser flash diffusivity (LFD).

TGA and DSC data were used to develop a decomposition model including reaction enthalpy. The LFD data indicated that the thermal diffusivity was constant, at least before significant mass loss. To extrapolate to higher temperatures, an effective thermal conductivity model was also developed to predict thermal conductivity of fully degraded MXB-71 at high temperatures. However, above 900°C, the material vitrifies and has significant volume changes.

The effective thermal conductivity model separates conductive heat transfer into three parts: conduction through the solid, conduction through the decomposition gases, and diffusive radiation. Most heat transfer occurs via conduction through the solid, since little mass is loss during decomposition. At 1000°C, the mass loss is 17% and the predicted gas volume fraction increases by 15%.

Observations and model

Table 1 shows a 5-step decomposition model based on the TGA, DSC, and LFD data for MXB-71 shown in Figure 1. The 4.9-mg TGA and the 13.5-mg DSC samples were heated at 20°C/minute, respectively. The TGA apparatus measures mass loss as the sample temperature increases. The solid mass (m) normalized by the initial sample mass (m_o), $S_f = m/m_o$, along with the derivative dS_f/dt are shown in Figure 1.A. Pictures of 1-mm thick cured LFD samples are shown on the mass loss curve at the corresponding cure temperatures and also in Figure 1.C. Significant volume changes and likely enthalpy changes occur above 725°C, which were not measured by the DSC experiment. Therefore, the MXB-71 chemistry model above 725°C should be used with caution.

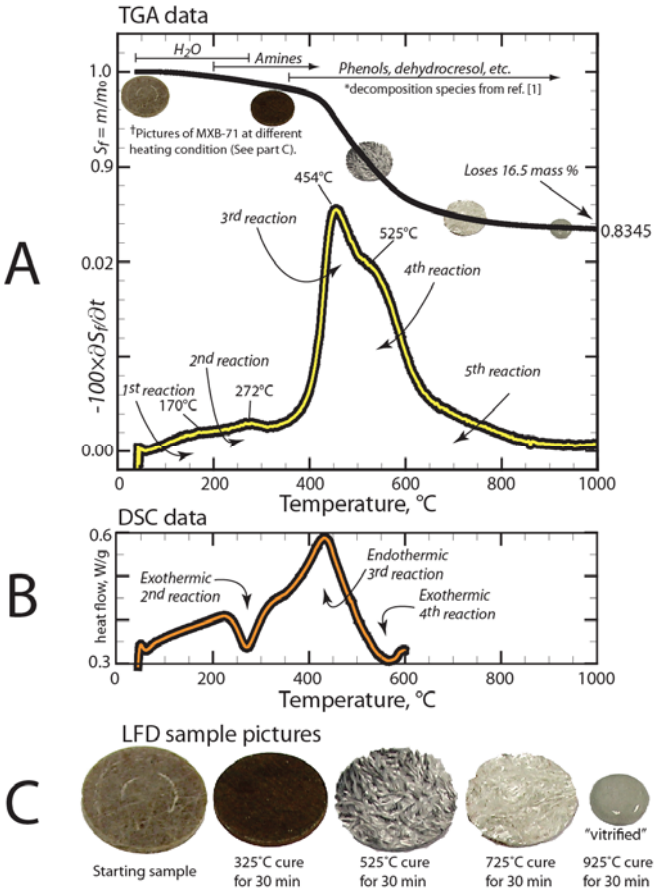

Figure 1. A) TGA, B) DSC, and C) LFD data.

The derivative in Figure 1.A indicates that four reactions centered about 170, 272, 454, and 525°C describe decomposition. A fifth reaction with the center obscured by the 3rd and 4th reactions could be used to describe the slope change at 650°C. Table 1 gives a five-step decomposition model with parameters that can accurately describe the mass loss in Figure 1.A.The DSC data in Figure 1.B suggests the first reaction is thermally neutral, the 2nd reaction is exothermic, the 3rd reaction is endothermic, the 4th reaction is exothermic, and the reaction enthalpy of the 5th reaction is uncertain. The 5th reaction is assumed to be thermally neutral although endothermic processes associated with vitrification are expected. More data beyond 600°C is needed to establish these enthalpy changes.

Table 1. Five step decomposition model with parameters.*

			Reactions: $C_i \rightarrow G_i$ i = 1,5				
Symbol	**Description**	**Units**	**1**	**2**	**3**	**4**	**5**
C_o	Initial concentration	mass fraction	0.010±5%	0.002±5%	0.023±5%	0.065±5%	0.066±5%
E/R	Normalized activation energy	K	20000	23000	29000	30000	34000
σ/R	Dispersion in activation energy	K	2000	200	300	1500	5500
Ln(A)	Natural logarithm of prefactors	Ln(s^{-1})	37.0	37.0	35.7	32.8	33.7
h	Reaction enthalpies	kJ/g (cal/g)	0	6.28 (1500)±5%	-1.67 (-400)±5%	1.38 (330)±5%	0
σ	Reaction rate uncertainty†	none	1±20%	1±20%	1±20%	1±20%	1±20%

* i represents species and reactions 1 through 5.

† The reaction rate uncertainty is 1±20% implemented as a rate multiplier.

The five reaction rates were distributed with respect to reaction extent: $r_i = \partial C_i/\partial t = \xi_i A_i \exp[(-E_i+z\sigma_i)/RT]C_i$ with z_i=**normsinv**$(1-C_i/C_{o,i})$. i represents the five reactions. The quantity, $(1-C_i/C_{o,i})$, represents the progress of the i^{th} reaction. **normsinv** returns the inverse of the standard normal cumulative distribution function.

Predictions of the TGA and DSC experiments

Figure 2 compares predicted and measured TGA mass loss and the DSC heat flow. The colored lines represent the mass loss and derivative of mass loss associated with the five independent reactions. The individual reacted mass loss fractions were determined by $S_{f,i}=1-G_i$. The sum of the individual reacted solid fractions is given by the solid black line, which is in agreement with the data represented by circles.

The derivatives of mass loss show that the first and last reactions are broad and do not show prominent peaks in the derivative curve, especially the last reaction. In contrast the 2nd, 3rd, and 4th reactions are narrower with distinct peaks. The second reaction does not contribute much to the mass loss, but helps capture the first exothermic reaction in Figure 2.B. This reaction occurs over a small temperature range and may be the curing agent burning off. Both the 1st and 5th reactions were assumed to have a net enthalpy change of zero. Heat flow was calculated as $q_{flow}=q_{sen}+q_{rxn}$, where $q_{sen}=C_p\partial T/\partial t$ with $q_{rxn}=\Sigma r_i q_i$. The overall reaction enthalpy (64 J/g) was determined as the difference between the integral of the sensible energy (dashed purple line) and the heat flow (solid black line).

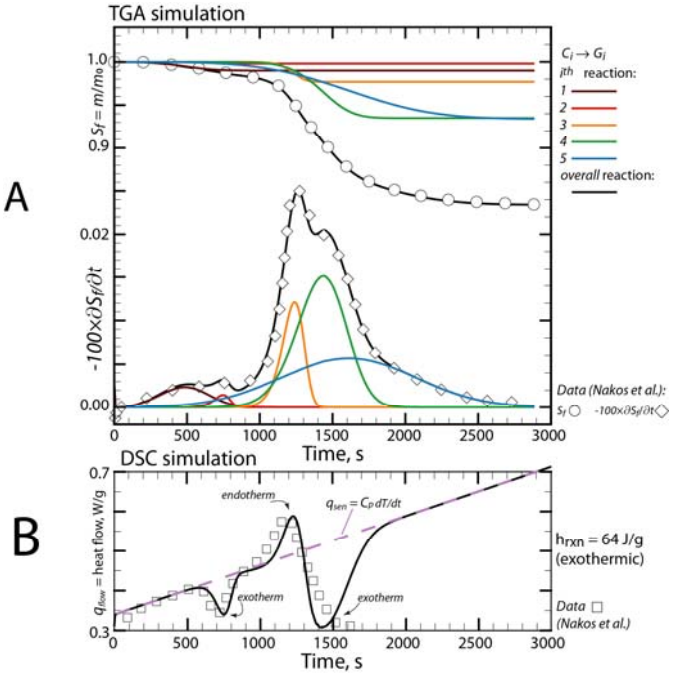

Fig. 2. TGA and DSC data (symbols) and predictions (lines).

MXB-71 response model

The response of the MXB-71 was determined with a finite element model (FEM) that solves the heat diffusion equation with a source term for chemistry, $\rho C_p \partial T/\partial t = \nabla\cdot(k_{eff}\nabla T)+\Sigma q_i r_i$, where ρ, C_p, T, t, k_{eff}, q, and r represent material density, specific heat, temperature, time, effective thermal conductivity, volumetric reaction energy, and reaction rate, respectively. The effective conductivity model is composed of gas conduction (k_g), condensed conduction (k_c), and diffusive radiation (k_r): $k_{eff} = k_g + k_c + k_r$. More details regarding the response model with parameters can be found in [2].

A sample calculation of MXB-71 confined in an 8.4-cm diameter by 4-cm high right circular cylinder (stainless steel) with a 2-cm diameter embedded hollow cylinder (aluminum) is shown in Figure 2. All external surfaces were assumed to be insulated except for the bottom plate which was heated from room temperature (27°C) to 1000°C in 10 minutes and held for an additional 400 s for a total heating time of 1000 s. Figure 2.A shows isotherms at 1000 s calculated with a 2D axisymmetric model. Figure 2.B shows the same isotherms using a 3D model and with identical results. Color is used in Figure 7.A and 7.B to depict gas volume fraction and reacted solid fraction, respectively.

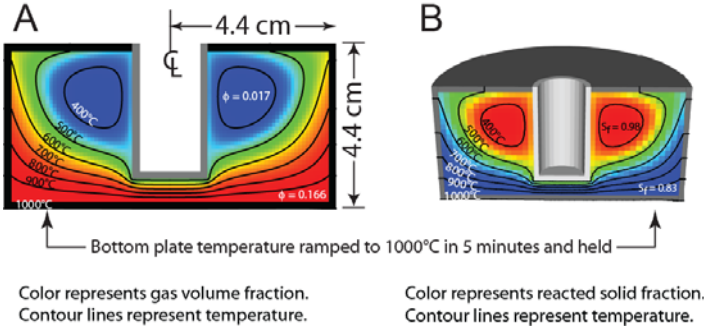

Fig. 3. Simulation of MXB-7 in can with hollow cylinder.

Conclusion

Five first-order reactions were used to simulate decomposition of MXB-71 using TGA, DSC, and LFD data. The reaction mechanism was implemented into a finite element code and a sample calculation performed. Component scale data is needed to validate the model.

Acknowledgements

Sandia is a multiprogram laboratory operated by Sandia Corporation, a Lockheed Martin Company, for the United States Department of Energy under Contract DE-AC04-94AL85000. We appreciate the experimental efforts of Ken Erickson, Walter Gill, John Oelfke, and Jill Suo-Anttila. We would also like to thank the internal reviewers of this memo, Tre' Shelton and Amanda Dodd.

References

1. Johnson R.T. Jr. and Biefeld R.M. *Polymer Engineering and Science*, **22** (3), 147 (1982).
2. Hobbs, M.L., Nakos, J.T., Brady, P. D. to be submitted to *J. Phys. Chem A.*